Neural effects of TMS trains on the human prefrontal cortex

Jessica M. Ross[2,1,3], Christopher C. Cline[1,3], Manjima Sarkar[1,3], Jade Truong[1,3], Corey J. Keller[1,2,3]*

[1]Department of Psychiatry and Behavioral Sciences, Stanford University Medical Center, 401 Quarry Road, Stanford, CA, 94305, USA

[2]Veterans Affairs Palo Alto Healthcare System, and the Sierra Pacific Mental Illness, Research, Education, and Clinical Center (MIRECC), 3801 Miranda Avenue, Palo Alto, CA 94304, USA

[3]Wu Tsai Neuroscience Institute, Stanford University, Stanford, CA, USA

*Correspondence:
Corey J. Keller, MD, PhD
Stanford University
Department of Psychiatry and Behavioral Sciences
401 Quarry Road
Stanford, CA 94305-5797
Email: ckeller1@stanford.edu
Phone: +1 8025786292

Running title. Neural effects of TMS trains

Abstract

Despite adoption of repetitive TMS (rTMS) for the treatment of neuropsychiatric disorders, a lack of understanding of its neural effects limits our ability to monitor, personalize, and adapt treatments. Here we address the methodological limitations in capturing the neural response to a single TMS train, the fundamental building block of treatment. We developed methods to measure these effects noninvasively and evaluated the acute neural response to single and sequential TMS trains. In 16 healthy adults, we applied 10 Hz trains to the dorsolateral prefrontal cortex (dlPFC) in a randomized, sham-controlled, event-related design and assessed changes to the TMS-evoked potential (TEP), a measure of local cortical excitability. We hypothesized that single TMS trains would induce changes in the local TEP amplitude that would accumulate across trains, but we found no evidence in support of this hypothesis. However, exploratory analyses demonstrated modulations non-locally and in phase and source space. Single and sequential TMS trains may not be sufficient to modulate the local TEP amplitude, but induce acute neural changes measured in alternative ways. This work should be contextualized as methods development for the monitoring of transient neural changes during rTMS and contributes to a growing understanding of the neural effects of rTMS.

Keywords. Non-invasive brain stimulation (NIBS); Transcranial magnetic stimulation (TMS); Electroencephalogram (EEG); Transcranial evoked potential (TEP)

Introduction

Repetitive transcranial magnetic stimulation (rTMS) is a safe and effective treatment for major depressive disorder, obsessive-compulsive disorder, smoking cessation, and migraines [1]. Despite FDA clearance for depression 15 years ago, one-month post-treatment response rates remain low at 50% [2,3]. This suboptimal response rate may in part be due to the fact that little is known about how rTMS treatment modulates neural activity in humans. Specifically, gaining a better understanding of how a single TMS train, the building block of rTMS treatment, modulates neural activity would provide foundational knowledge to guide the next generation of treatments. For example, development of an acute neural indicator of single TMS trains demonstrating prefrontal target engagement could guide high throughput screening of novel TMS patterns and lead to adaptive, closed loop TMS treatments.

Unlike other noninvasive modalities, the TMS-EEG evoked potential (TEP) provides a causal measurement of local cortical excitability [4–11] and thus is well suited for probing the neural effects of TMS trains. While a few motor cortex studies have explored the acute neural effects of rTMS, showing TEP modulation within 55-100 ms of a TMS train [12–14], little to no work to date has focused on the dlPFC, critical for treatment of psychiatric disorders. Furthermore, numerous large non-brain artifacts confound the TEP in this >50 ms time window [15–18]. Previous work in our lab demonstrated that short-latency neural responses at 25 and 33 ms may increase more following 10, 15, or 20 Hz trains compared to 1 Hz trains (manuscript under review). Critically, this study examined the evoked responses directly following a TMS train (within 300 ms). This approach is difficult to interpret because of the strong sensory responses lasting up to 300 ms after the last pulse in the train. As such, in order to account for these sensory confounds, and to deliver a causal measure of brain excitability, we evaluated post-train effects using extra single TMS pulses at latencies of greater than 300 ms after the last pulse in the train.

We focus on the early (< 80 ms) components of the TEP as our primary outcome measures due to their relationship to local excitability [19,20] and clinical outcome [7,19]. The earliest TEP peaks are suppressed after rTMS treatment for depression [19], distinguish between patients with depression and healthy control subjects [20], and the degree of these early TEP changes relate to clinical outcome [7,19]. Current TMS-EEG evidence suggests that the early TEP is free of confounding sensory responses [16–18,21,22]. A similar early neural response is observable in invasive investigations following single electrical pulses, further validating that this part of the TEP can be non-sensory [23].

In the current study, we sought to evaluate the acute neural effects of single and sequential dlPFC TMS trains using a sham-controlled, event-related study design. We hypothesized that single TMS but not sham trains would modulate acute cortical excitability, captured in the early local TEP, and that sequential TMS trains would lead to accumulated effects in the early local TEP. However, we found no evidence for single train or cumulative train effects on the early local TEP size when observed in sensor space. In contrast, exploratory analyses revealed that single trains induced non-local TEP effects and modulations in both oscillatory phase dynamics [24–26] and source estimates. This work should be contextualized as methods development for the monitoring of transient neural changes during rTMS and contributes to a growing understanding of the neural effects of rTMS.

Methods

Participants. This study was approved by the Stanford University Institutional Review Board. 52 healthy participants (19-65 years old [M=44.4, SD=13.3, 31F/20M/1O]) responded to an online

recruitment and after an initial online screening and consent, 18 eligible participants (25-60 years old [M=42.9, SD=11.8, 9F/9M]) were enrolled. Two participants withdrew because rTMS was intolerable and the remaining 16 participants were included in the analyses (M=43.1 years, SD=12.5, 8F/8M). See Table S1 for more demographics.

Inclusion criteria on the online screening form were (a) aged 18-65, (b) able to travel to study site, (c) fluent in English and (d) fully vaccinated against COVID-19. Exclusion criteria were (a) lifetime history of psychiatric or neurological disorder, (b) substance or alcohol abuse/dependence in the past month, (c) heart attack in the past 3 months, (d) pregnancy, (e) presence of any contraindications for rTMS, such as history of epileptic seizures or certain metal implants [27], or (f) psychotropic medications that increase risk of seizures including Bupropion (=>300mg/day) and/or any dose of Clozapine. Participants were also required to complete the *Quick Inventory of Depressive Symptomatology (16-item, QIDS)* self-report questionnaire and were excluded from the study if they scored 11 or higher indicating moderate depression [28,29]. All participants completed an MRI pre-examination screening form provided by the Richard M. Lucas Center for Imaging at Stanford University to ensure participant safety prior to entering the MRI scanner. Eligible participants were scheduled for two study visits: an anatomical MRI scan on the first visit and a TMS-EEG session on the second visit.

Overall study design. Conditions were chosen to examine the transient neural effects induced after single and sequential 10 Hz TMS trains were applied to the left dlPFC. We quantified transient induced neural effects using the TMS-evoked potential (TEP) evoked by single pulses of TMS (*probe pulses*) applied after each train (Fig 1A). We chose to quantify the effects of TMS trains in this manner to obtain a causal measurement of train-induced neural effects and because TEPs are well described in the literature [7,30]. Because the sensory response to TMS pulses lasts for at least 300 ms [15,21,22,31,32], we chose to add a 500 ms delay between the last pulse in the TMS train and the first TMS *probe pulse* . Because we hypothesized that the neural effects of single TMS trains would be transient and not last longer than one second, and to examine the temporal specificity of the effects, we applied a second *control* probe pulse two seconds after the TMS train. While it would have been advantageous to probe the acute neural effects less than 500 ms after the TMS train, we determined that strong sensory responses to the TMS train and the inability to perfectly match the perception of active and sham rTMS would render interpretation of a TEP < 500 ms after a TMS train extremely difficult. For four subjects, we jittered probe latencies within early (500-700 ms) and later (1900-2100 ms) latency time windows to evaluate if the neural effects observed at 500 ms and 2 s were dependent on those exact timings (Fig S4). Given the lack of clear neural effects between TEP responses after probe pulses applied within each jittered 200 ms range (Fig S4), for subsequent subjects we focused experimentation on the neural effects at fixed (500 ms and 2 s) probe times following the TMS train.

Our main outcome measure was the TEP from each probe pulse following TMS and sham trains. Changes in the TEPs were quantified by examining the early (20-50 ms and 50-80 ms) time windows of the TEP from EEG electrodes underneath the TMS brain target in the four conditions: (1) TEP from the probe pulse 500 ms after an active TMS train (*active rTMS, early probe*); (2) TEP from the probe pulse 2000 ms after an active TMS train (*active rTMS, late probe*); (3) TEP from the probe pulse 500 ms after a sham TMS train (*sham rTMS, early probe*); (4) TEP from the probe pulse 2000 ms after a sham TMS train (*sham rTMS, late probe*). To explore the cumulative effects of sequential TMS trains on the TEP, for each condition 12 consecutive TMS trains were applied in block order for N=13 subjects. The order of conditions was randomized. We hypothesized that single 10 Hz trains to the dlPFC would affect the early (20-50 ms) local TEP for less than one second following active TMS trains (active rTMS early probe would be different than

all other conditions). We further hypothesized that sequential TMS trains would enhance this effect.

Transcranial magnetic stimulation.

TMS targeting and calibration. Both single pulse TMS and TMS trains were delivered using a MagVenture Cool-B65 A/P figure-of-eight coil (MagVenture, Denmark) from a MagPro X100 system (MagVenture, Denmark). A thin (0.5 mm) foam pad was attached to the TMS coil to minimize electrode movement and bone-conducted auditory artifact. A TMS-Cobot-2 system (Axilum Robotics, France) was used to automatically maintain orientation of the active coil relative to the subject's head. Neuronavigation (Localite TMS Navigator, Alpharetta, GA) was used to derive the TMS targets for each subject based on their individual T1-weighted MRI image. MRI was performed on a GE DISCOVERY MR750 3-T MR system (General Electric, Boston, Massachusetts) using a 32 channel head coil. T1 structural scans were acquired using a BRAVO pulse sequence (T1-weighted, sagittal slice thickness 1 mm, acquisition matrix 256 $\times$ 256, TR 8 ms, TE 3 ms, FA 15°).

Resting motor threshold. To obtain resting motor threshold (RMT), single pulses of TMS were delivered to the hand region of the left motor cortex with the coil held tangentially to the scalp and at 45° from the mid-sagittal plane. The optimal motor hotspot was defined as the coil position from which TMS produced the largest and most consistent visible twitch in a relaxed first dorsal interosseous (FDI) muscle. RMT was determined to be the minimum intensity that elicited a visible twitch in relaxed FDI in ≥ 5/10 stimulations.

Determining target location, coil angle, and intensity. Our goal was to maximally modulate the left dlPFC node of the fronto-parietal network with TMS. Thus, we targeted a set of MNI coordinates (-38, 23, 38) previously identified as the group (N=38) peak of that node within the fronto-parietal network [33]. To minimize discomfort, we applied single pulses of TMS at 110% RMT at various angles (0°, 45°, and 90°) from the mid-sagittal plane and instructed subjects to select the angle that was most tolerable [22]. The optimal angle for each subject can be found in Table S2. Each subject then underwent a TMS train intensity ramp to introduce the sensation of the train and subjects were instructed to notify operators if stimulation intensity became intolerable. The first TMS train began at 55% RMT and gradually increased to 110% RMT. In cases of intolerance, the stimulation intensity was adjusted down until tolerable for the following TMS train blocks (Table S2 for tolerable intensity used for each participant). Two participants found the TMS trains to be intolerable at all intensities and withdrew their participation.

Repetitive TMS (active rTMS). We applied 10 Hz TMS trains for 5 s (50 pulses). Each TMS train was followed by a first single pulse probe at 500 ms (*early probe*) and a second single pulse probe at 2000 ms (*late probe*), as defined in the previous section and depicted in Fig 1B. Probe TMS pulses were always 'active', regardless of whether they were preceded by an active or sham TMS train. Stimulation was arranged in 16 blocks, with each block including 24 TMS trains equally split between 12 sequential active trains and 12 sequential sham trains. A 10 minute rest period was placed after every 4 blocks, and a 1 minute rest period between all other blocks.

Sham repetitive TMS (sham rTMS). In order to quickly switch between active and sham TMS trains, we used a dual coil approach (Fig S12). The active TMS coil was placed over the left dlPFC while the sham coil was positioned over the right dlPFC. The sham coil was a MagVenture Cool-B65 A/P coil with the sham-side facing the scalp and fixed in place using a coil holder. Electrical current was delivered during sham TMS trains over the left frontalis muscle, using two surface electrodes (Ambu Neuroline 715) in order to approximate the somatosensory sensations arising from skin mechanoreceptors and scalp muscles during the active TMS condition [34]. We posited

that although the sham TMS coil was placed over the right hemisphere, the electrical stimulation would be felt over the left hemisphere under the active TMS coil, and the auditory click from the sham TMS coil would reach bilateral auditory cortices with similar timing and intensity as from the active TMS coil. Electrical current stimulation intensity was calibrated to approximate the scalp sensation and discomfort of active TMS. To assess how closely matched the active and sham rTMS sensations were, subject perceptual ratings of loudness, scalp sensation, and pain were collected and analyzed (as described in more detail in Analyses).

Electroencephalography. 64-channel EEG was obtained using a BrainVision actiCHamp Plus amplifier, with ActiCAP slim active electrodes in an extended 10–20 system montage (actiCHamp, Brain Products GmbH, Munich, Germany). EEG data were online referenced to Cz and recorded using BrainVision Recorder software v1.24.0001 (Brain Products GmbH, Germany). Impedances during TMS-EEG studies were monitored and percentage of channels with impedances <10 kΩ was 94.38 ∓ 6.75%. Electrode locations were digitized using Localite (Localite TMS Navigator, Alpharetta, GA).

Analyses

All EEG preprocessing and analyses were performed in MATLAB R2021a (Mathworks, Natick, MA, USA) using the EEGLAB v2021.1 toolbox [35] and custom scripts. TMS-EEG preprocessing was performed with version 2 of the AARATEP pipeline [36], with source code available at github.com/chriscline/AARATEPPipeline. Data were processed in batches grouped by 4 sequential blocks (each batch containing probe responses from 48 real trains and 48 sham trains) to account for artifact changes that may occur over the duration of one session[37]. Epochs were extracted from 350 ms before to 1100 ms after each TMS probe pulse.

As part of the AARATEP pipeline v2, the following steps were taken, with details described in Cline *et al.* (2021) [36]. Data between 2 ms before to 12 ms after the pulse were replaced with values interpolated by autoregressive extrapolation and blending, downsampled to 1 kHz, and baseline-corrected based on mean values between 350 to 10 ms before the pulse. Epochs were then high-pass filtered with a 1 Hz cutoff frequency and a modified filtering approach to reduce spread of artifact into baseline time periods. Bad channels were rejected via quantified noise thresholds and replaced with spatially interpolated values (see Cline *et al.*, 2021 [36] for all details on channel deletion and interpolation). Eye blink artifacts were attenuated using a dedicated round of independent-component analysis (ICA) and eye-specific component labeling and rejection using ICLabel [38]. Various non-neuronal noise sources were attenuated with SOUND [39]. Decay artifacts were reduced via a specialized decay fitting and removal procedure. Line noise was attenuated with a bandstop filter between 58-62 Hz. Additional artifacts were attenuated with a second stage of ICA and ICLabel component labeling and rejection, with rejection criteria targeted at removing any clearly non-neural signals (see Cline *et al.*, 2021 [36] for all data deletion criteria). Data were again interpolated between -2 ms and 12 ms with autoregressive extrapolation and blending, low-pass filtered with a cutoff frequency of 100 Hz, and re-referenced to the average.

TMS train effects on the TEP. To compare single pulse TMS responses from probes at 500 and 2000 ms after active and sham TMS trains, we computed the local mean field amplitude (LMFA) for 20-50 ms and 50-80 ms time windows in a dlPFC region of interest (ROI). Because apparent amplitude of an averaged EEG waveform is not independent of latency variance, and the early TEP peaks are not yet well defined, we used a metric (area under the curve, AUC) to capture the full morphology of the LMFA waveform by aggregating the LMFA waveform over a time window rather than focusing on an instantaneous amplitude [40,41]. We chose these time windows following

5

Gogulski *et al.* (2023)[42] and because they are far enough after the interpolated time window (ending at 12 ms) and before time windows that are reported to include strong off-target sensory effects [16,21,22]. The early 20-50 ms time window captures our primary hypothesized component of interest, the early local TEP. The later 50-80 ms time window captures other TEP components that have been previously reported in both prefrontal[42] and motor cortex [43–45]. The local ROI was chosen to cover the stimulation site and left lateral prefrontal cortex broadly: AF3, F7, F5, F3, F1, FC3. Using a within subjects design, the LMFA measurement from each time window (20-50 ms, 50-80 ms) was entered as a dependent variable into a repeated measures analysis of variance (ANOVA) with probe latency (early 500 ms probe, late 2000 ms probe) and stimulation (active TMS train, sham TMS train) factors. To test if TMS trains modulated neural activity in downstream regions, we repeated the above-described analysis using right frontal, left parietal, and right parietal ROIs.

Sequential TMS train effects on the TEP. We examined the relationship between TMS train order (in the 12 train sequence) and the post-train TEPs. To reduce dimensions, TEPs were averaged over groupings of three adjacent trains in the 12-train sequence (trains 1-3, 4-6, 7-9, and 10-12). To assess effects of TMS train sequence on the TEP, a repeated measures ANOVA was performed across these four train groupings. Three subjects did not have 12 sequential trains, so N=13 subjects were included in this analysis.

Exploratory analyses.
Sensor space hierarchical linear modeling (LIMO). As an exploratory investigation of condition-specific responses with minimal assumptions about relevant ROIs or time windows, we used the Hierarchical LInear MOdeling of ElectroEncephaloGraphic Data (LIMO EEG) toolbox [46]. First-level beta parameters for each channel and time window were estimated from TEP features with ordinary least squares. Second-level analysis used a 2✕2 repeated measures ANOVA (early probe, late probe; active rTMS, sham rTMS), with cluster-based correction for multiple comparisons (bootstrap N=1000, alpha = 0.05).

Phase space reconstructions using recurrence quantification analysis (RQA). EEG complexity due to oscillatory phase shifting can be quantified using recurrence quantification analysis (RQA; see [26] for a review), a nonlinear analysis of phase behavior in dynamical systems [23,24]. In RQA, a time series is compared to itself with a predefined lag time to isolate phase regularity, visualized using a recurrence plot, and parameters are calculated to quantify phase regularity. For this analysis we used the local ROI and a 15 ms lag time to capture phase dynamics relevant to early local TEP peaks such as N15-P30-N45. The RQA parameter Percent Determinism measures predictability in the phase structure of a time series. This parameter was selected due to relevance for neural circuit coordination and for distinguishing between coordination stability regimes [47]. RQA was performed on early and late probe and active and sham rTMS conditions (delay = 15 ms, embedding dimension = 6, range = -80 to 80 ms). Percent determinism was calculated using all trials and compared across the conditions with a 2✕2 repeated measures ANOVA (active rTMS, sham rTMS; early probe, late probe).

Source space estimates. Subject-specific differences in gyral anatomy can cause underlying common cortical sources to project to the scalp in different topographies across subjects[48]. To account for this and other related consequences of EEG volume conduction, we performed EEG source estimation. Using digitized electrode locations and individual head models constructed from subjects' anatomical MRI data[49], subject-specific forward models of signal propagation from dipoles distributed over and oriented perpendicular to the cortical surface to electrodes on the scalp were constructed [50,51]. One subject did not have digitized electrode locations available, so

was excluded from the source analysis (N=15). Inverse kernels mapping measured scalp EEG activity to underlying cortical sources were estimated using weighted minimum-norm estimation (wMNE) as implemented in Brainstorm[52]. Surface-based morphometry was used to map activations from subject-specific cortical surfaces to a common group template surface (ICBM152). A data-driven process was used to identify source-space spatial filters based on observed peaks in the average source TEP responses aggregated from data pooled across all subjects and stimulation conditions. Response amplitudes were then extracted by applying these latency-specific spatial filters to subject- and condition-specific data subsets. For each identified TEP latency of interest, a 2✕2 repeated measures ANOVA was used to assess effects of stimulation (active rTMS, sham rTMS) and probe latency (early probe, late probe).

Sensory perception of TMS trains and single pulse TMS probes. To assess how closely matched the active and sham conditions actually were, subject perceptual ratings of loudness, scalp sensation, and pain were collected and analyzed. Prior to the experimental conditions, participants were asked to provide perceptual ratings after each of seven stimulation conditions: (1) single pulse TMS with no preceding train, (2) active TMS train with no probe pulse, (3-4) early probe at 500 ms and late probe at 2000 ms after an active TMS train, (5) sham TMS train with no probe pulse, and (6-7) early probe at 500 ms and late probe at 2000 ms after a sham TMS train. The order of these conditions were randomized across participants but with single pulse TMS being applied before all TMS train conditions for all participants. As performed previously in Ross *et al.* (2022)[22], participants were instructed to respond verbally immediately following each stimulation to rate *loudness, scalp sensation,* and *pain perception* on scales ranging from 0 to 10. To ensure consistency in how these questions were phrased across conditions and subjects, scripts were used following Ross *et al.* (2022)[22].

Statistical analyses of perceptual ratings. Perceptual ratings were compared between active and sham conditions (active vs. sham rTMS, early probe after active vs. early probe after sham rTMS, late probe after active vs. late probe after sham rTMS) using nine paired t-tests for loudness perception, scalp feeling, or pain ratings. Multiple comparisons were corrected for using the Bonferroni type adjustment.

Results

Effects of TMS trains on TEPs. First we asked whether there was a significant change in the local sensor-space TEP after different types of TMS trains (active vs. sham) and using different probe latencies after the TMS train (500 ms, 2000 ms). Single trains of left dlPFC TMS did not evoke neural effects on the TEP using this analysis (Fig 1B-E, N = 16). For the first peak in the early local TEP (20-50 ms, LMFA, Fig 1E and S1-S2), we observed an effect of probe latency ($F_{(1,15)}$=10.2000, p=0.0060) but no effect of stimulation ($F_{(1,15)}$=0.9735, p=0.3395), and no probe latency by stimulation interaction ($F_{(1,15)}$=3.1384, p=0.1000). For the second peak in the early local TEP (50-80 ms, Fig 1E and S1-S2), we observed no effect of probe latency ($F_{(1,15)}$=4.2198, p=0.0578) and no effect of stimulation ($F_{(1,15)}$=2.2449, p=0.1548). See Figs S1-S2 for individual TEP waveforms across conditions. To confirm this null effect was not due to the specific latency chosen between the TMS train and probe pulses, four subjects with jittered early probe latencies (500-700ms) were evaluated; we found no significant effect on TEP response. See Fig S4 for more details on this analysis. To verify that these results were not due to the type of quantification performed (LMFA), we repeated the analysis using peak to peak amplitudes (in dB) and observed no main effect of probe latency ($F_{(1,9)}$=0.5255, p=0.4869) and no main effect of stimulation ($F_{(1,9)}$=0.9619, p=0.3523; see Fig S13). In summary, active TMS trains did not differ from sham trains in eliciting effects early and local to the site of stimulation.

To investigate potential downstream modulation from 10 Hz trains, we next quantified the effects of probe latency and stimulation type on TEPs using the global mean field amplitude (GMFA, uses all electrodes) and in regions of interest (ROIs) farther from the site of stimulation (right frontal, left parietal, right parietal; Fig 2, N = 16). Using all electrodes (GMFA), we observed an effect of probe latency (Fig 2C, E; 500 ms vs. 2000 ms; $F(1,15)=7.2050$, $p=0.0170$) but no effect of stimulation (Fig 2C, E; active vs. sham TMS trains; $F(1,15)=3.1534$, $p=0.0961$), and no probe latency by stimulation interaction ($F(1,15)=4.2375$, $p=0.0573$). In the right frontal ROI, we observed an effect of probe latency ($F(1,15)=7.8531$, $p=0.0134$), an effect of stimulation ($F(1,15)=6.0103$, $p=0.0270$), and no interaction between probe latency and stimulation ($F(1,15)=1.4014$, $p=0.2549$). In the left parietal ROI, we found no effect of probe latency ($F(1,15)=2.1164$, $p=0.1663$) and no effect of stimulation ($F(1,15)=4.4061$, $p=0.0531$). In the right parietal ROI, we found an effect of probe latency ($F(1,15)=5.3080$, $p=0.0360$), but no effect of stimulation ($F(1,15)=0.7821$, $p=0.3904$), and no interaction ($F(1,15)=2.3411$, $p=0.1468$) See Fig 2D,F for more details, and supplementary for individual subject GMFA (Fig S5) and downstream LMFA time series (Figs S6-S8). In summary, we observed main stimulation effects of TMS trains that represent a reduction in TEP size in the right frontal ROI, without clear effects in GMFA or other downstream ROIs tested.
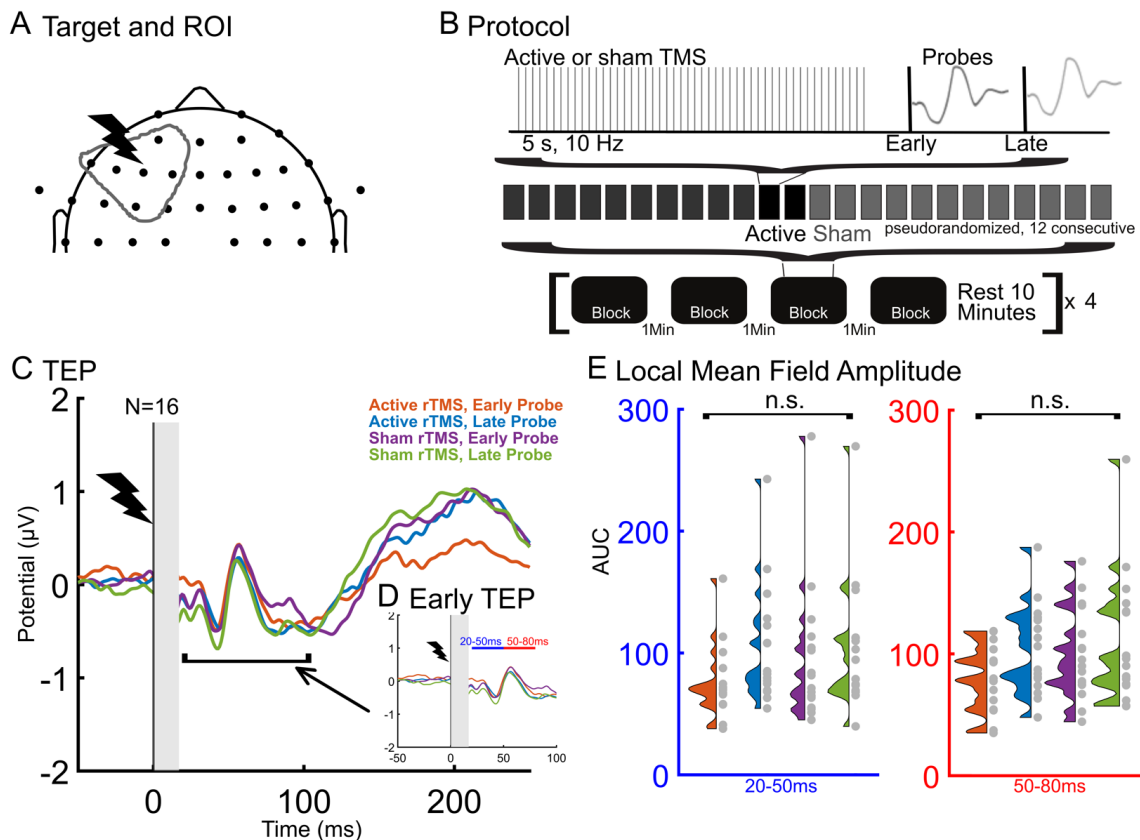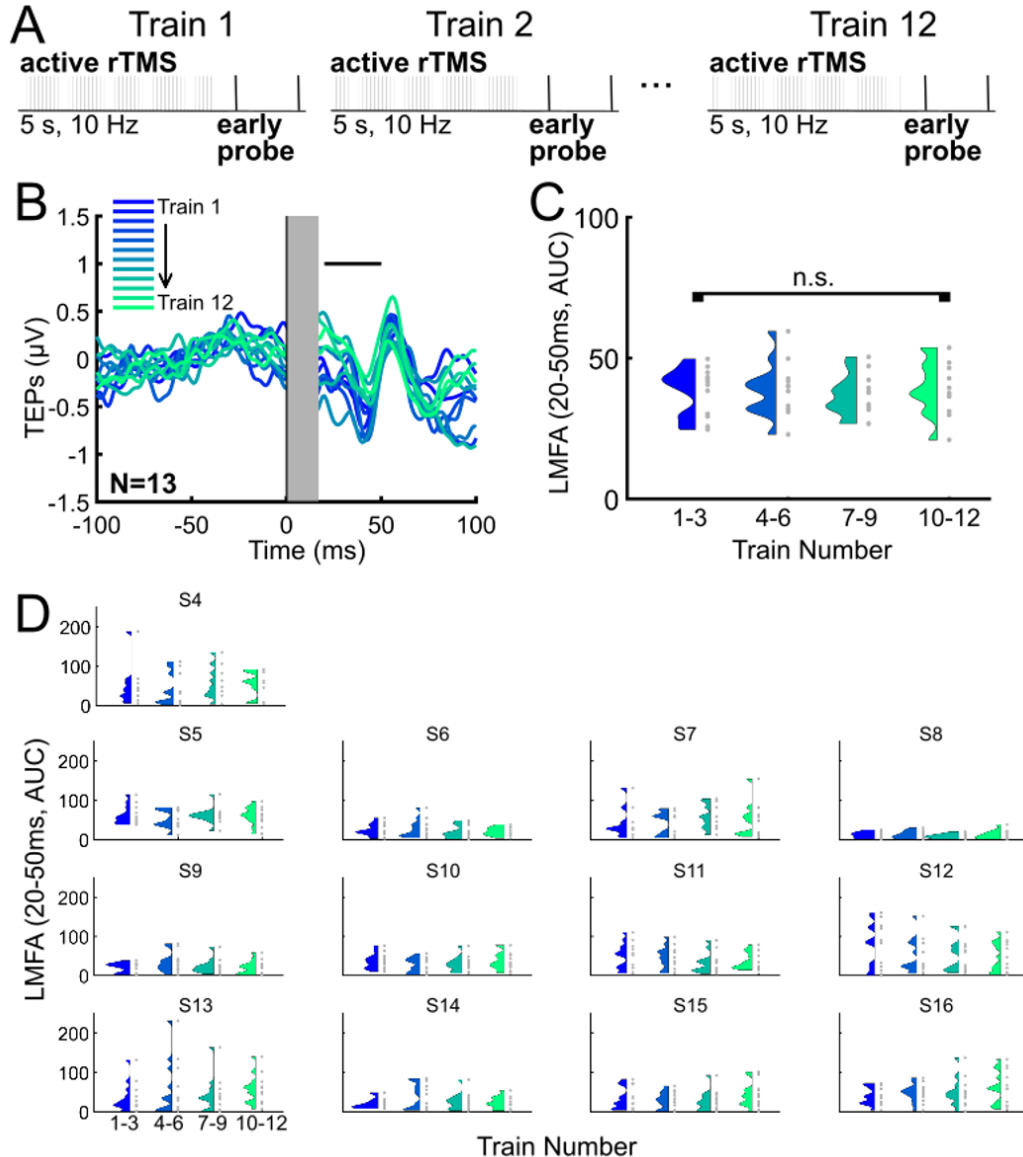

Figure 1. TMS trains did not modulate early local TEP when observed in sensor space. A) TMS was delivered over the left dlPFC and local TEP analysis was performed using six left frontal electrodes. B) Experimental design: Active and sham TMS trains were applied to the left dlPFC and single TMS pulses were used as probes to evaluate the TMS-evoked potential (TEP). Probe pulses were applied at 500ms (*early probe*) to assess early rTMS-induced changes or 2s (*late probe*) as a control. All probe pulses were active TMS, allowing a direct comparison between active and sham trains. To assess cumulative inter-train effects, up to 12 consecutive active and sham trains were applied. The blocks of active or sham rTMS were randomized. C) Group TEP (N=16) shown for the -50ms to 250ms window. Time = 0 is the time of the single TMS probe pulse. D) Early TEP (N=16) with the two analysis latency windows indicated with blue (20-50 ms) and red (50-80 ms) horizontal bars. See Supplementary for individual subject LMFA time series (Fig S1-S2). E) Group effects of the local TEP in two time windows across conditions.
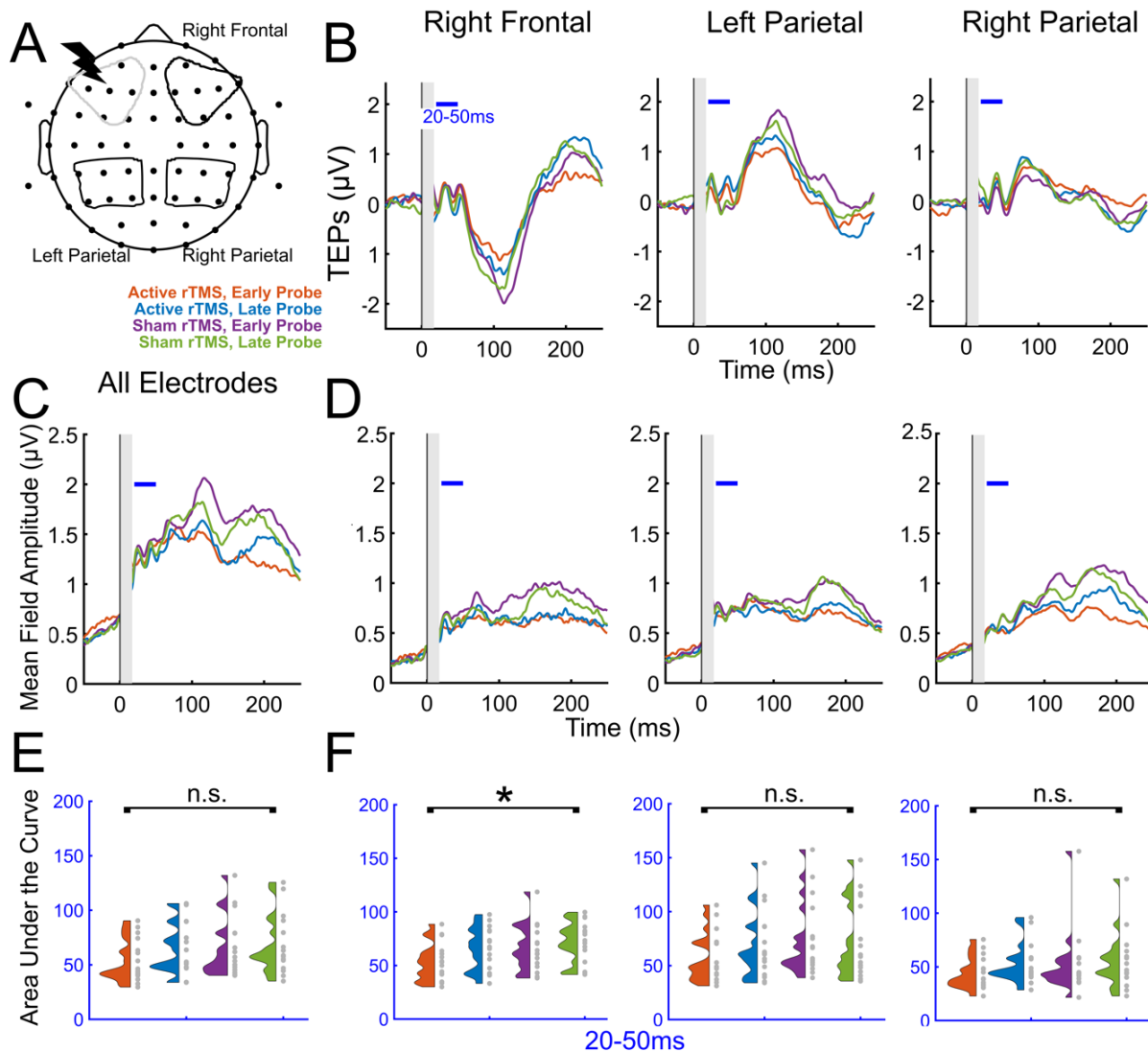
Figure 2. TMS trains reduce cortical excitability in a right frontal ROI. A) Regions of interest for TEP analyses. B-F) Comparisons of TEP conditions using all electrodes (GMFA) and downstream ROIs (LMFA). B) Group TEPs (N=16) for each ROI, with analysis latency windows indicated with a blue (20-50 ms) horizontal bar. C) Group averaged global mean field amplitude for all electrodes (N=16). D) Group average local mean field amplitude for downstream ROIs. E) Individual subject global mean field amplitude area under the curves in the four conditions, calculated using the 20-50 ms TEP latency window. F) Group LMFA across conditions, calculated using the 20-50 ms TEP latency window. See Supplementary S5-S8 for individual subjecttime series and results from both 20-50 ms and 50-80 ms time windows. Main effects of stimulation are indicated with an asterisk (*p<0.05).

Sequential TMS train effects on the TEP. Next we asked if repeated 10 Hz trains elicited cumulative neural effects, assessed by sequential TEP measurements (Fig 3, N=13). We observed no cumulative effects on the early local TEP after up to 12 sequential TMS trains. See figure 3B-C for the first peak of the early local TEP (20-50 ms window; $F_{(3,36)}=0.4340$, $p=0.7300$) and figures 3B and S9 for the 50-80 ms window ($F_{(3,36)}=0.7722$, $p=0.5172$). For an additional follow-up analysis of later TEP time windows 80-130 ms (Fig S10) and 130-250 ms (Fig S11), see Supplementary Materials. In summary, we did not observe a group effect of sequential TMS trains on the TEP.

Figure 3. Sequential TMS trains did not modulate the local TEP. A) In this study, 12 sequential active and sham TMS trains were applied, each followed by an early probe at 500 ms (also see Fig 1B). B) Group average (N=13) TEP from the early probe following each sequential active TMS train, with the early latency window indicated with a black (20-50 ms) horizontal bar. C) Group average TEP response from the early probe following each sequential active TMS train. TEPs are grouped based on the order of the associated TMS train (groupings of three consecutive trains). D) Individual subject TEP results from the early probe following sequential active TMS trains. For the 50-80 ms TEP window see Fig S9. For later latencies see Figs S10-S11.
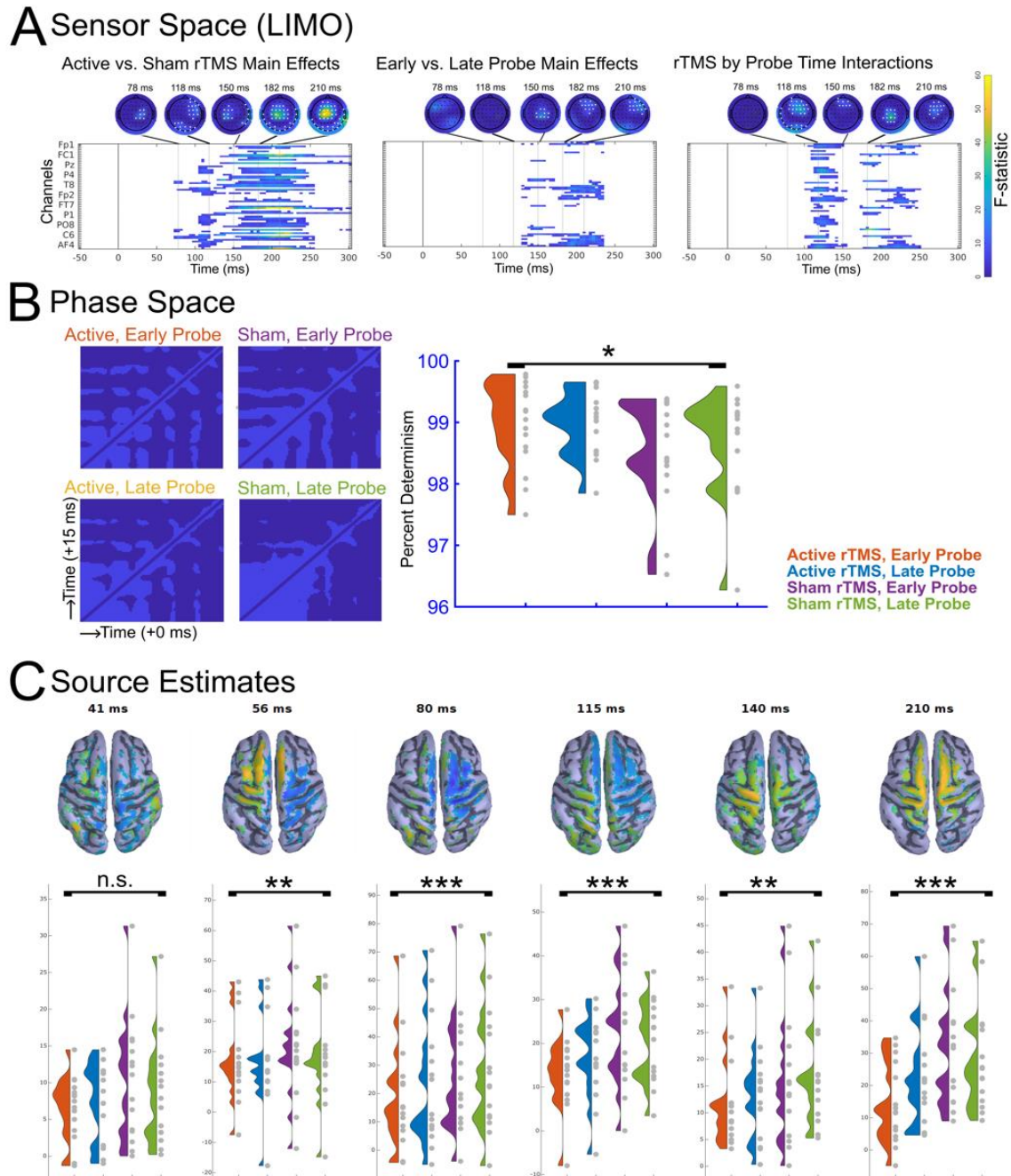
Exploratory analyses.

Sensor space hierarchical linear modeling (LIMO). As an exploratory investigation of condition-specific responses with minimal assumptions about relevant ROIs or time windows, we used the LIMO toolbox [46]. LIMO analyses revealed significant effects of stimulation (active vs. sham), of probe latency (early vs. late), and significant interactions between these two factors (Fig 4A). The most prominent effects were observed at later latencies, especially between 100-250 ms, at central and bilateral frontal scalp electrodes.

10

Phase space reconstructions using recurrence quantification analysis (RQA). EEG complexity due to oscillatory phase shifting was quantified using RQA [24–26]. This analysis on percent determinism revealed significant effects of stimulation ($F_{(1,15)} = 5.2452$, p = 0.0369), no main effects of probe latency ($F_{(1,15)} = 0.3869$, p = 0.5433), and no stimulation by probe latency interactions ($F_{(1,15)} = 0.4596$, p = 0.5082). Percent determinism was greater with active than with sham TMS trains, regardless of probe latency (Fig 4B, N=16, recurrence plots show t=0 ms and 15 ms).

Source space estimates. Cortical source activity was averaged across all stimulation conditions and subjects (Fig 4; data-driven spatial filters derived in Fig 4C and response amplitudes Fig 4D). 2×2 repeated-measures ANOVAs were performed on eight peak times present in the source response amplitudes. We found main effects of stimulation at latencies spanning 56-210 ms (56 ms $F_{(1,14)}=12.077$, p=0.00371; 80 ms $F_{(1,14)}=21.576$, p=0.000379; 115 ms $F_{(1,14)}=17.442$, p=0.000932; 140 ms $F_{(1,14)}=14.045$, p=0.00216; 210 ms $F_{(1,14)}=39.473$, p=0.0000201), a main effect of probe latency at 140 ms ($F_{(1,14)}=4.837$, p=0.0452), and stimulation by probe latency interactions at 115 ms ($F_{(1,14)}=13.502$, p=0.00250) and 210 ms ($F_{(1,14)}=18.302$, p=0.000765). In summary, active rTMS reduced the TEP at latencies spanning 56-210 ms, there was a main effect of probe latency at 140 ms indicating that early probes resulted in smaller potentials than late probes, and at 115 and 210 ms there were also stimulation by probe latency interactions indicating that the stimulation-related reduction in TEP at these peaks was a function of probe latency. See figure S14 for more details and figure S15 for all individual subject source estimate time series and topographies.

Sensory perception of TMS trains and single pulse TMS probes. To better understand how well matched the sensory experiences were between active and sham conditions, we compared the perceptual ratings (Fig S3) using paired t-tests. These nine tests were corrected for multiple comparisons, resulting in an adjusted α of 0.0056. With respect to isolated active vs. sham TMS trains, we observed no statistical differences in loudness perception ($t(15) = 3.8776$, p = 0.0015), pain ($t(15) = 1.0274$, p = 0.3205), or scalp sensation ($t(15) = 3.0138$, p = 0.0087). When testing the perception of the probe pulses following active vs. sham TMS trains, we observed no effects across all conditions, including loudness perception (early probe, $t(15) = 2.6112$, p = 0.0197; late probe, ($t(15) = 2.3342$, p = 0.0339), scalp sensation (early probe, $t(15) = 3.0138$, p = 0.0186; late probe, $t(15) = 2.893$, p = 0.112), and pain (early probe, $t(15) = 2.9084$, p = 0.0108; late probe,$t(15) = 3.0382$, p = 0.0083)). The only comparison that resulted in statistically significant differences was loudness perception between active and sham TMS trains ($t(15) = 3.8776$, p = 0.0015), indicating that the active TMS trains were perceived to be louder than the sham trains. These results suggest that the perception of scalp feeling and pain were relatively well matched between active and sham conditions, that auditory loudness perception was indistinguishable across different probe latencies within train conditions, but that loudness perception was unmatched between active and sham TMS trains.

Figure 4. Exploratory analyses revealed that TMS trains modulate the non-local late TEP, early local TEP phase dynamics, and source estimates across both early and late TEP. A) LIMO analysis (N=16) F-statistic heatmaps and topographies, corrected for multiple comparisons. Electrodes with F-statistics surpassing the significance threshold are shown in white. B) RQA recurrence plots averaged over all subjects (N=16) showing t(0ms) by t(15ms) and group averages of percent determinism by condition (lag = 15 ms, embedding dimensions = 6). C) Source estimates for condition specific TEPs (N=15) with topographies and group averages shown at 6 peak times determined from the averaged source TEP. For more details, see Fig S14. Main effects of stimulation are indicated with asterisks (*p<0.05, **p<0.01, ***p<0.001).

12

Discussion

In this study we sought to evaluate whether 10 Hz TMS trains to the dlPFC induce acute neural effects quantifiable in the early local TEP. Due to the well-described sensory responses to TMS, which we also observed after each pulse within a train, we applied the probe single pulses at latencies that should be clear of train-evoked sensory potentials. We found that: 1) prefrontal TMS trains did not induce acute neural changes in the size of the early TEP in regions local to the stimulation site, 2) up to 12 sequential TMS trains did not elicit a cumulative effect on these early local TEPs, but that 3) in exploratory analysis TMS trains did induce neural changes in the non local TEP, early local oscillatory phase dynamics, and source estimates across multiple TEP latencies. In the context of previous work[12,13,36], these findings indicate that although TMS trains did not modulate neural excitability in the prefrontal cortex, findings observed during exploratory analysis have important implications for the direction of future work.

Sequential TMS train effects on the TEP. Because it is generally accepted that when enough TMS trains are applied to the dlPFC there are lasting neural changes, we hypothesized that sequential TMS trains may induce changes in cortical excitability that accumulate as a function of TMS train. We observed that up to 12 sequential TMS trains was not sufficient to induce cumulative neural changes in the early TEP measured locally to the site of stimulation. Several possible explanations exist: 1) 12 trains represents only ~1/6 of a standard TMS treatment for depression and thus is not sufficient to modulate cortical excitability; 2) 12 trains is sufficient but changes in cortical excitability is non-linear and thus the analytic choice is not ideal; 3) low signal-to-noise in the TEP reduced the ability to detect change; 4) 12 trains is sufficient in depression but not in healthy participants. Regardless of the reason, future work is needed to tease apart this critical question. We are developing a better understanding of how the signal-to-noise of the TEP differs as a function of dlPFC subarea[42] and are now developing fully personalized methods to minimize artifact and boost signal. We are developing methods to better match the perceptual effects of active and sham TMS trains so that small neural changes in active compared to sham are more easily detected and attributed to direct effects and not differences in sensory perception. Future work will continue to investigate this important question about neural changes from sequential TMS trains by applying more TMS trains in a row.

Non-local effects of TMS trains. We find that TMS trains modulate cortical excitability in downstream brain regions. Specifically, we observed neural modulation after 10 Hz TMS trains in the right frontal ROI (Fig 2B-F). To investigate further, we used the LIMO tool, which is particularly well-suited for exploratory investigations of all EEG spatial and temporal information [46]. The strength of this approach is for hypothesis generation starting with minimal assumptions about relevant ROIs or time windows. We observed TMS-induced modulation in downstream regions, most clearly at the scalp vertex and along the midline. These modulations occur at latencies later than our predefined early TEP time window. Considering the suggested role of inhibitory influences in this later time window [21], these results may be interpreted to mean that our TMS protocol modulated inhibitory contributions to the TEP. However, due to the known sensory-related vertex potential that occurs within this same time window [16,21,22], these results may also be interpreted to indicate perceptual differences between the experimental conditions. Our further analysis in source space supports the presence of modulation across multiple latencies spanning 56-210ms. However, these modulations were mostly not localized to the site of stimulation, which could be explained by greater inter-individual variability in early latency response morphologies, modulation of distributed circuits connected to the stimulation site, or sensory effects. If it is the case that there are components in this time window that are inhibitory in nature, our data support that suppression of these components was strongest for early probes after active rTMS (Fig 4C),

13

suggesting that the acute effects of TMS trains were a reduction of inhibition in downstream brain networks.

Early local phase dynamics of TMS trains. To address the possibility that the TEP is not suited for capturing rTMS-induced phase shifting behavior of single or sequential trains, we applied a dynamical systems method for quantifying changes in phase space of time series that consist of oscillatory signals, RQA [24]. This method was used here to determine if RQA can be used to capture neural phase modulation induced by 10 Hz TMS trains. One strength of RQA is that it can robustly measure complexity of a signal that is short duration and non-stationary, as in short recordings of human EEG [53–58]. We found evidence that TMS trains have quantifiable effects on EEG phase dynamics – that phase of the early local TEP has more determinism following active 10 Hz TMS trains than following sham trains. This indicates increased complexity following TMS trains. Specifically, high determinism can be indicative of metastable or multistable coordination dynamics as in multifunctional neural coordination[47] and this analysis indicates that TMS trains may induce these dynamics in TMS affected neuronal populations [24,47]. This dynamical systems approach will be valuable in future investigations aimed at mechanistic understanding of the induced neural changes with single and also with repeated trains, which is not possible using TEP amplitudes alone. Therefore, we suggest that dynamical systems approaches should be incorporated into future work on TMS mechanism. Due to the exploratory nature of the RQA analysis in this study, these mechanistic interpretations should be vetted in future work specifically focused on TEP phase shifting regimes.

Limitations and future directions. Other possibilities for the null effects from single or multiple trains on TEP amplitudes are related to our methodological decisions. First, the exact probe latencies of 500 and 2000 ms may not have been ideal to capture neural effects. In a subsample of subjects, we explored if jittering the early and late probe latencies from 500-700 ms and from 1900-2100 ms, respectively, had a clear influence on early local TEP modulation, but we did not find evidence for this. Secondly, it is possible that the early probe was not applied close enough to the end of the train to capture induced TEP amplitude changes. Unfortunately, using earlier probes would result in TEPs that are confounded by sensory artifacts from the last pulse in the train. Unless active and sham TMS trains are perfectly matched perceptually, the neural effects when placing the early probe closer to the TMS train would be difficult to interpret. Although our primary results were null, findings from our exploratory analyses indicated that the design used in this study was sufficient to capture induced TEP modulation in downstream brain regions, in phase dynamics, and in source estimates. In future work, train effects should be understood as synchronization of excitatory and inhibitory neural activity in prefrontal cortex and connected networks. Future work should explore the EEG signal following rTMS as a dynamical system with phase shifting behavior in order to develop mechanistic understandings of rTMS modulations and to detect dynamic oscillatory changes not visible using TEP amplitudes. Ongoing work in our lab will further explore the induced complexity in neural modulations. In other future work, this train-probe approach described here will be used to evaluate the neural effects of TMS trains applied across frequencies (e.g. 1 Hz, 20 Hz), patterns (iTBS, cTBS), train duration, inter-train intervals, and train intensity. Most importantly, future work should also explore whether this experimental approach can be used for real-time measurement of monitoring the neural effects of TMS trains. If successful, this real-time approach has important implications in developing closed-loop adaptive TMS treatments[59].

Conclusions

We evaluated the neural effects of single and sequential 10 Hz TMS trains to the left prefrontal cortex using single 'probe' TMS pulses. We found that single prefrontal TMS trains did not modulate prefrontal cortical excitability when compared to sham TMS trains. We also did not

observe cumulative neural changes following 12 sequential TMS trains. However, exploratory analyses suggest that single TMS trains induced non-local cortical excitability changes, changes in phase space, and changes using source space models. This work provides important groundwork for future directions and highlights the experimental complexity required to measure acute neural changes to TMS treatment.

References

1. Chail, A., Saini, R. K., Bhat, P. S., Srivastava, K. & Chauhan, V. Transcranial magnetic stimulation: A review of its evolution and current applications. *Ind Psychiatry J* **27**, 172–180 (2018).
2. Blumberger, D. M. *et al.* Effectiveness of theta burst versus high-frequency repetitive transcranial magnetic stimulation in patients with depression (THREE-D): a randomised non-inferiority trial. *The Lancet* **391**, 1683–1692 (2018).
3. Trevizol, A. P. *et al.* Predictors of remission after repetitive transcranial magnetic stimulation for the treatment of major depressive disorder: An analysis from the randomised non-inferiority THREE-D trial. *EClinicalMedicine* **22**, 100349 (2020).
4. Stefanou, M.-I. *et al.* Brain State-dependent Brain Stimulation with Real-time Electroencephalography-Triggered Transcranial Magnetic Stimulation. *JoVE* 59711 (2019) doi:10.3791/59711.
5. Zrenner, B. *et al.* Brain oscillation-synchronized stimulation of the left dorsolateral prefrontal cortex in depression using real-time EEG-triggered TMS. *Brain Stimulation* **13**, 197–205 (2020).
6. Zrenner, C., Desideri, D., Belardinelli, P. & Ziemann, U. Real-time EEG-defined excitability states determine efficacy of TMS-induced plasticity in human motor cortex. *Brain Stimulation* **11**, 374–389 (2018).
7. Eshel, N. *et al.* Global connectivity and local excitability changes underlie antidepressant effects of repetitive transcranial magnetic stimulation. *Neuropsychopharmacol.* **45**, 1018–1025 (2020).
8. Ilmoniemi, R. J. *et al.* Neuronal responses to magnetic stimulation reveal cortical reactivity and connectivity: *NeuroReport* **8**, 3537–3540 (1997).
9. Ilmoniemi, R. J. & Kičić, D. Methodology for Combined TMS and EEG. *Brain Topogr* **22**, 233–248 (2010).
10. Ozdemir, R. A. *et al.* Cortical responses to noninvasive perturbations enable individual brain fingerprinting. *Brain Stimulation* **14**, 391–403 (2021).
11. Rogasch, N. C. & Fitzgerald, P. B. Assessing cortical network properties using TMS-EEG. *Hum. Brain Mapp.* **34**, 1652–1669 (2013).
12. Esser, S. K. *et al.* A direct demonstration of cortical LTP in humans: A combined TMS/EEG study. *Brain Research Bulletin* **69**, 86–94 (2006).
13. Hamidi, M., Slagter, H. A., Tononi, G. & Postle, B. R. Brain responses evoked by high-frequency repetitive transcranial magnetic stimulation: an event-related potential study. *Brain Stimul* **3**, 2–14 (2010).
14. Veniero, D., Maioli, C. & Miniussi, C. Potentiation of short-latency cortical responses by high-frequency repetitive transcranial magnetic stimulation. *J Neurophysiol* **104**, 1578–1588 (2010).
15. Conde, V. *et al.* The non-transcranial TMS-evoked potential is an inherent source of ambiguity in TMS-EEG studies. *NeuroImage* **185**, 300–312 (2019).
16. Biabani, M., Fornito, A., Mutanen, T. P., Morrow, J. & Rogasch, N. C. Characterizing and minimizing the contribution of sensory inputs to TMS-evoked potentials. *Brain Stimulation* **12**, 1537–1552 (2019).
17. Rocchi, L. *et al.* Disentangling EEG responses to TMS due to cortical and peripheral activations. *Brain Stimulation* **14**, 4–18 (2021).
18. Freedberg, M., Reeves, J. A., Hussain, S. J., Zaghloul, K. A. & Wassermann, E. M. Identifying site- and stimulation-specific TMS-evoked EEG potentials using a quantitative cosine similarity metric. *PLoS ONE* **15**, e0216185 (2020).

19. Voineskos, D. *et al.* Neurophysiological effects of repetitive transcranial magnetic stimulation (rTMS) in treatment resistant depression. *Clin Neurophysiol* **132**, 2306–2316 (2021).

20. Voineskos, D. *et al.* Altered Transcranial Magnetic Stimulation-Electroencephalographic Markers of Inhibition and Excitation in the Dorsolateral Prefrontal Cortex in Major Depressive Disorder. *Biol Psychiatry* **85**, 477–486 (2019).

21. Ross, J. M. *et al.* A structured ICA-based process for removing auditory evoked potentials. *Sci Rep* **12**, 1391 (2022).

22. Ross, J. M., Sarkar, M. & Keller, C. J. Experimental suppression of transcranial magnetic stimulation - electroencephalography sensory potentials. *Human Brain Mapping* hbm.25990 (2022) doi:10.1002/hbm.25990.

23. Keller, C. J. *et al.* Induction and Quantification of Excitability Changes in Human Cortical Networks. *J. Neurosci.* **38**, 5384–5398 (2018).

24. Richardson, M., Paxton, Alexandra, & Kuznetsov, Nikita. Nonlinear methods for understanding complex dynamical phenomena in psychological science. in *APA Psychological Science Agenda* (2017).

25. Richardson, M. J., Schmidt, R. C. & Kay, B. A. Distinguishing the noise and attractor strength of coordinated limb movements using recurrence analysis. *Biol Cybern* **96**, 59–78 (2007).

26. Marwan, N. A historical review of recurrence plots. *Eur. Phys. J. Spec. Top.* **164**, 3–12 (2008).

27. Rossi, S., Hallett, M., Rossini, P. M. & Pascual-Leone, A. Screening questionnaire before TMS: An update. *Clinical Neurophysiology* **122**, 1686 (2011).

28. Yeung, A. *et al.* The Quick Inventory of Depressive Symptomatology, clinician rated and self-report: a psychometric assessment in Chinese Americans with major depressive disorder. *J Nerv Ment Dis* **200**, 712–715 (2012).

29. Rush, A. J. *et al.* The 16-Item Quick Inventory of Depressive Symptomatology (QIDS), clinician rating (QIDS-C), and self-report (QIDS-SR): a psychometric evaluation in patients with chronic major depression. *Biol Psychiatry* **54**, 573–583 (2003).

30. Ilmoniemi, R. J. & Kičić, D. Methodology for Combined TMS and EEG. *Brain Topogr* **22**, 233–248 (2010).

31. Nikouline, V., Ruohonen, J. & Ilmoniemi, R. J. The role of the coil click in TMS assessed with simultaneous EEG. *Clinical Neurophysiology* **110**, 1325–1328 (1999).

32. Gordon, P. C., Desideri, D., Belardinelli, P., Zrenner, C. & Ziemann, U. Comparison of cortical EEG responses to realistic sham versus real TMS of human motor cortex. *Brain Stimulation* **11**, 1322–1330 (2018).

33. Chen, A. C. *et al.* Causal interactions between fronto-parietal central executive and default-mode networks in humans. *Proceedings of the National Academy of Sciences* **110**, 19944–19949 (2013).

34. Gordon, P. C. *et al.* Recording brain responses to TMS of primary motor cortex by EEG - utility of an optimized sham procedure. *Neuroimage* **245**, 118708 (2021).

35. Delorme, A. & Makeig, S. EEGLAB: an open source toolbox for analysis of single-trial EEG dynamics including independent component analysis. *Journal of Neuroscience Methods* **134**, 9–21 (2004).

36. Cline, C. C., Lucas, M. V., Sun, Y., Menezes, M. & Etkin, A. Advanced Artifact Removal for Automated TMS-EEG Data Processing. in *2021 10th International IEEE/EMBS Conference on Neural Engineering (NER)* 1039–1042 (IEEE, 2021). doi:10.1109/NER49283.2021.9441147.

37. Rogasch, N. C., Biabani, M. & Mutanen, T. P. Designing and comparing cleaning pipelines for TMS-EEG data: A theoretical overview and practical example. *Journal of Neuroscience Methods* **371**, 109494 (2022).

38. Pion-Tonachini, L., Kreutz-Delgado, K. & Makeig, S. ICLabel: An automated electroencephalographic independent component classifier, dataset, and website. *Neuroimage* **198**, 181–197 (2019).

39. Mutanen, T. P., Metsomaa, J., Liljander, S. & Ilmoniemi, R. J. Automatic and robust noise suppression in EEG and MEG: The SOUND algorithm. *NeuroImage* **166**, 135–151 (2018).

40. Beauchemin, M. & De Beaumont, L. Statistical analysis of the mismatch negativity: To a dilemma, an answer. *TQMP* **1**, 18–24 (2005).

41. Kappenman, E. S. & Luck, S. J. Best Practices for Event-Related Potential Research in Clinical Populations. *Biol Psychiatry Cogn Neurosci Neuroimaging* **1**, 110–115 (2016).

42. Gogulski, J. *et al. Mapping cortical excitability in the human dorsolateral prefrontal cortex.* http://biorxiv.org/lookup/doi/10.1101/2023.01.20.524867 (2023) doi:10.1101/2023.01.20.524867.

43. Tremblay, S. *et al.* Clinical utility and prospective of TMS-EEG. *Clin Neurophysiol* **130**, 802–844 (2019).

44. Kähkönen, S., Komssi, S., Wilenius, J. & Ilmoniemi, R. J. Prefrontal transcranial magnetic stimulation produces intensity-dependent EEG responses in humans. *NeuroImage* **24**, 955–960 (2005).

45. Lioumis, P., Kičić, D., Savolainen, P., Mäkelä, J. P. & Kähkönen, S. Reproducibility of TMS-Evoked EEG responses. *Hum. Brain Mapp.* **30**, 1387–1396 (2009).

46. Pernet, C. R., Chauveau, N., Gaspar, C. & Rousselet, G. A. LIMO EEG: a toolbox for hierarchical LInear MOdeling of ElectroEncephaloGraphic data. *Comput Intell Neurosci* **2011**, 831409 (2011).

47. Kelso, J. A. S. Multistability and metastability: understanding dynamic coordination in the brain. *Philos Trans R Soc Lond B Biol Sci* **367**, 906–918 (2012).

48. Michel, C. M. & Murray, M. M. Towards the utilization of EEG as a brain imaging tool. *NeuroImage* **61**, 371–385 (2012).

49. Thielscher, A., Antunes, A. & Saturnino, G. B. Field modeling for transcranial magnetic stimulation: A useful tool to understand the physiological effects of TMS? in *2015 37th Annual International Conference of the IEEE Engineering in Medicine and Biology Society (EMBC)* 222–225 (IEEE, 2015). doi:10.1109/EMBC.2015.7318340.

50. Gramfort, A., Papadopoulo, T., Olivi, E. & Clerc, M. OpenMEEG: opensource software for quasistatic bioelectromagnetics. *BioMed Eng OnLine* **9**, 45 (2010).

51. Kybic, J. *et al.* A common formalism for the Integral formulations of the forward EEG problem. *IEEE Trans. Med. Imaging* **24**, 12–28 (2005).

52. Tadel, F., Baillet, S., Mosher, J. C., Pantazis, D. & Leahy, R. M. Brainstorm: A User-Friendly Application for MEG/EEG Analysis. *Computational Intelligence and Neuroscience* **2011**, 1–13 (2011).

53. Heunis, T. *et al.* Recurrence quantification analysis of resting state EEG signals in autism spectrum disorder – a systematic methodological exploration of technical and demographic confounders in the search for biomarkers. *BMC Med* **16**, 101 (2018).

54. Bhat, S., Acharya, U. R., Adeli, H., Bairy, G. M. & Adeli, A. Automated diagnosis of autism: in search of a mathematical marker. *Reviews in the Neurosciences* **25**, (2014).

55. Pistorius, T., Aldrich, C., Auret, L. & Pineda, J. Early Detection of risk of autism spectrum disorder based on recurrence quantification analysis of electroencephalographic signals. in *2013 6th International IEEE/EMBS Conference on Neural Engineering (NER)* 198–201 (IEEE, 2013). doi:10.1109/NER.2013.6695906.

56. Acharya, U. R., Sree, S. V., Chattopadhyay, S., Yu, W. & Ang, P. C. A. Application of recurrence quantification analysis for the automated identification of epileptic EEG signals. *Int. J. Neur. Syst.* **21**, 199–211 (2011).

57. Song, I.-H., Lee, D.-S. & Kim, S. I. Recurrence quantification analysis of sleep electoencephalogram in sleep apnea syndrome in humans. *Neuroscience Letters* **366**, 148–153 (2004).

58. Becker, K. *et al.* Anaesthesia Monitoring by Recurrence Quantification Analysis of EEG Data. *PLoS ONE* **5**, e8876 (2010).

59. Parmigiani, S. *et al.* Reliability and validity of TMS-EEG biomarkers. *Biological Psychiatry: Cognitive Neuroscience and Neuroimaging* S2451902222003408 (2022) doi:10.1016/j.bpsc.2022.12.005.

Author contributions. JMR, CC, and CJK conceptualized and designed the study, with significant contributions from MS and JT. CC programmed the experiment. MS and JT collected the data. JMR, CC, and MS conducted the analyses. All authors interpreted the results. All authors contributed to the writing of the manuscript. All authors provided intellectual contributions to and approval of the final manuscript.

Supplementary Information. The online version contains supplementary material.

Correspondence and requests for materials should be addressed to C.J.K.